

# Stability and structure of two coupled boson systems in an external field

T. Sogo, O. Sørensen, A.S. Jensen, and D.V. Fedorov

*Department of Physics and Astronomy, University of Aarhus, DK-8000 Aarhus C, Denmark*

(Dated: February 2, 2008)

The lowest adiabatic potential expressed in hyperspherical coordinates is estimated for two boson systems in an external harmonic trap. Corresponding conditions for stability are investigated and the related structures are extracted for zero-range interactions. Strong repulsion between non-identical particles leads to two new features, respectively when identical particles attract or repel each other. For repulsion new stable structures arise with displaced center of masses. For attraction the mean-field stability region is restricted due to motion of the center of masses.

PACS numbers: 31.15.Ja, 21.45.+v, 05.30.Jp

*Introduction.* Bose-Einstein condensation is by now routinely realized in many laboratories [1, 2]. Static and dynamic properties are currently investigated by use of Feshbach resonances to manipulate the effective two-body interactions. Two-component and mixed systems open for a variety of combinations. Two-component condensed bosons systems consisting of the same atoms in different spin states are formed [3, 4] and collective oscillations studied for  $^{87}\text{Rb}$  [5]. Condensates of two different species were recently created combining  $^{87}\text{Rb}$  and  $^{41}\text{K}$  [6]. Also mixed systems of condensed boson and degenerate fermions was recently experimentally obtained [7].

Theoretical descriptions often use the mean-field approximation with zero range interactions [1, 2]. Both stability and average properties are successfully described for one-component boson systems which so far are the most intensively studied. The simplest model for two-component and mixed systems is a coupled mean-field approximation [8, 9, 10]. Two-cluster features may then be accounted for by using mean-field intrinsic and relative coordinates. However, for such systems a more complicated cluster structure may be favorable corresponding to lower energy. Competing or maybe co-existing new types of structures may appear. The stability conditions may be altered when degrees of freedom beyond the mean field are allowed.

The mean-field models are unable to investigate effects of correlations [11]. Correlations can be studied in hyperspherical models, which have been applied to one-component symmetric boson systems in external fields [12]. An extension to two-component systems requires at least introduction of a relative and a size coordinate for each subsystem. Compared to a one-component system the difficulties increase substantially. Therefore, before embarking on such a large project, it is advisable and illuminating to study the decisive large-distance limit with zero-range interactions and simple approximate wave functions. The purpose of the present letter is to provide estimates for conditions of stability and occurrence of new structures for two coupled boson systems.

*Theoretical method.* The  $N$  bosons have masses  $m_i$  and coordinates  $\vec{r}_i$ . We assume a division into two systems,  $A$  and  $B$ , of identical bosons with particle numbers  $N_A$  and  $N_B$  ( $N = N_A + N_B$ ) and total masses

$M_A \equiv N_A m_A$  and  $M_B \equiv N_B m_B$  ( $M \equiv M_A + M_B$ ). We shall use hyperspherical coordinates with the hyper-radius defined by [12, 13]

$$m\rho^2 \equiv \frac{1}{M} \sum_{i<j}^N m_i m_j r_{ij}^2 = \sum_{i=1}^N m_i r_i^2 - MR^2, \quad (1)$$

where  $m$  is an arbitrary normalization mass,  $\vec{r}_{ij} = \vec{r}_i - \vec{r}_j$  and  $\vec{R} = \sum_i m_i \vec{r}_i / M$  is the center-of-mass coordinate. The remaining degrees of freedom are described by the hyperangles collectively denoted by  $\Omega$ . A system divided into two different subsystems of non-identical particles requires independent parameters for each component. The size coordinates defined as the corresponding two hyper-radii are then the natural choice analogous to mean-field coordinates for each component. In addition we also allow the correlations corresponding to relative motion of the two center of masses. This is the minimum number of parameters for a two-component system where the sizes and center of mass positions can be independently varied. Thus we define the hyperradii and center-of-mass coordinates for the two systems  $A$  and  $B$

$$\rho_A^2 \equiv \frac{1}{N_A} \sum_{i<j}^{N_A} r_{ij}^2, \quad \rho_B^2 \equiv \frac{1}{N_B} \sum_{N_A < i < j}^N r_{ij}^2, \quad (2)$$

$$\vec{R}_A = \frac{1}{N_A} \sum_{i=1}^{N_A} \vec{r}_i, \quad \vec{R}_B = \frac{1}{N_B} \sum_{i=N_A+1}^N \vec{r}_i. \quad (3)$$

The average separation of the two components is then given by the coordinate  $\vec{r} \equiv \vec{R}_A - \vec{R}_B$ . The three length coordinates,  $\rho_A$ ,  $\rho_B$ , and  $r$ , are related to  $\rho$  by

$$m\rho^2 = m_A \rho_A^2 + m_B \rho_B^2 + m_r r^2, \quad m_r \equiv \frac{M_A M_B}{M_A + M_B}. \quad (4)$$

We aim at using the hyperspherical adiabatic expansion method. We only include the first adiabatic angular wave function, i.e.

$$\Psi = \rho_A^{2-3N_A/2} \rho_B^{2-3N_B/2} r^{-1} f(\rho_A, \rho_B, r) \Phi(\Omega), \quad (5)$$

where the separable center-of-mass motion is removed. We first assume that  $s$ -waves dominate in the angular

expansion and second that  $\Phi$  is independent of the angles. Then the wave function is automatically symmetric under permutations of particles within each subsystem. These assumptions are severe, but not unreasonable for spatially extended dilute systems.

The three short-range interactions are all chosen as  $\delta$ -functions with strengths expressed in terms of the corresponding two-body scattering lengths  $a_A$ ,  $a_B$ , and  $a_{AB}$ , i.e.

$$V_A = \sum_{i < j=1}^{N_A} g_A \delta^{(3)}(\vec{r}_{ij}), \quad g_A = \frac{4\pi\hbar^2 a_A}{m_A}, \quad (6)$$

$$V_B = \sum_{N_A < i < j=1}^N g_B \delta^{(3)}(\vec{r}_{ij}), \quad g_B = \frac{4\pi\hbar^2 a_B}{m_B}, \quad (7)$$

$$V_{AB} = \sum_{i=1}^{N_A} \sum_{j=N_A+1}^N g_{AB} \delta^{(3)}(\vec{r}_{ij}), \quad g_{AB} = \frac{2\pi\hbar^2 a_{AB}}{\mu_{AB}} \quad (8)$$

where  $\mu_{AB} \equiv m_A m_B / (m_A + m_B)$ . Integrating these interactions over all hyperangles we arrive at the Schrödinger equation which determines  $f$  in Eq. (5), i.e.

$$\left( -\frac{\hbar^2}{2m_A} \frac{\partial^2}{\partial \rho_A^2} - \frac{\hbar^2}{2m_B} \frac{\partial^2}{\partial \rho_B^2} - \frac{\hbar^2}{2m_r} \frac{\partial^2}{\partial r^2} + U_{eff} - E \right) f(\rho_A, \rho_B, r) = 0, \quad (9)$$

where the adiabatic effective potential for  $N_A \gg 1$  and  $N_B \gg 1$  is

$$\begin{aligned} \frac{2m_A}{\hbar^2} U_{eff}(\rho_A, \rho_B, r) = & \frac{\rho_A^2}{b_t^4} + \frac{m_B \rho_B^2}{m_A b_t^4} + \frac{m_r r^2}{m_A b_t^4} \\ & + \frac{9N_A^2}{4\rho_A^2} + \frac{9m_A N_B^2}{4m_B \rho_B^2} + \frac{3^{3/2}}{2\pi^{1/2}} \left( \frac{N_A^{7/2} a_A}{\rho_A^3} + \frac{m_A a_B N_B^{7/2}}{m_B \rho_B^3} \right. \\ & \left. + \frac{m_A (N_A N_B)^{7/4} a_{AB}}{\mu_{AB} (\rho_A \rho_B)^{3/2}} I(\rho_A, \rho_B, r) \right), \end{aligned} \quad (10)$$

where we have defined the trap length for the external-field frequency  $\omega$  as  $b_t^2 \equiv \hbar / (m_A \omega)$ . The dimensionless function  $I$  depends on  $N_A$ ,  $N_B$ ,  $\rho_A/r$ , and  $\rho_B/r$ . It arises from the angular average of the interaction  $V_{AB}$  between the particles in systems  $A$  and  $B$ .

*Effective potential.* The effective potential  $U_{eff}$  in Eq. (10) consists of three types of terms, i.e. from the external field (first three), the generalized centrifugal barrier (next two), and the angular average of the interactions and kinetic energies (last three). In total,  $U_{eff}/(\hbar\omega)$  depends on the particle numbers  $N_A$  and  $N_B$ , the ratio  $m_A/m_B$ , three coordinates and three scattering lengths measured in units of  $b_t$ .

The function  $I$  in Eq. (10) is a double integral with rather simple properties, i.e. it is monotonous as function of  $r$ , it vanishes when  $r > \rho_A + \rho_B$ , has a positive maximum and vanishing first derivative at  $r = 0$ , and it is unity when  $N_A = N_B$  and  $\rho_A = \rho_B$ .

The behavior of  $U_{eff}$  is qualitatively different for attractive and repulsive two-body interactions. The interaction terms ( $\rho^{-3}$ ) dominate for small distances, and for

strong attraction  $U_{eff}$  has no minimum. The system is always spatially confined by the external harmonic field. When subsystems  $A$  and  $B$  are identical, the effective potential has a local minimum when  $N|a|/b_t < 0.67$  [1, 2]. For asymmetric systems the corresponding stability conditions are more complicated, as we shall see.

To illustrate, we show in Fig. 1 for three repulsive scattering lengths the minimum of  $U_{eff}$  with respect to  $\rho_A$  and  $\rho_B$  as a function of  $r$  and various divisions of the total particle number 40000. For symmetric divisions coinciding centers of mass ( $r = 0$ ) are preferred. As the asymmetry increases ( $N_B < 0.134N_A$ ), a deeper minimum develops at finite  $r$ -values comparable to the trap length. The minimum at  $r = 0$  remains stable because the barrier separating the minima is much higher than the zero-point motion in both wells. The deepest minimum occurs for the asymmetric system with  $N_B/N_A \approx 1/40$ .

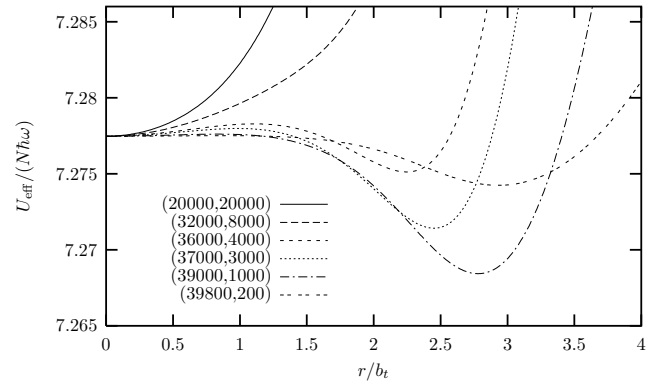


FIG. 1: The effective potential in Eq. (10) as a function of  $r/b_t$  for  $^{87}\text{Rb}$  masses  $m_A = m_B = 1.44 \times 10^{-25} \text{ kg}$ , trap length  $b_t = 2.22 \mu\text{m}$  ( $\omega = 2\pi \times 23.5 \text{ Hz}$ ), particle numbers  $N = N_A + N_B = 40000$ , and  $a_A = a_B = a_{AB} = 103a_0$ , where  $a_0$  is the Bohr radius. The curves correspond to the different values of  $(N_A, N_B)$  given on the figure.

*Structure.* The basic characteristics of a system are size and energy. The root-mean-square distance  $r_A$  is the measure of the size of system  $A$  defined by

$$N_A \bar{r}_A^2 \equiv \left\langle \sum_i^{N_A} (\vec{r}_i - \vec{R}_A)^2 \right\rangle = \langle \rho_A^2 \rangle, \quad (11)$$

where  $\langle \rangle$  denotes an expectation value. Correspondingly we define mean distances  $\bar{r}$  and  $\bar{r}_B$  for the total and the  $B$ -system, i.e.  $N\bar{r}^2 = \langle \rho^2 \rangle$  and  $N_B \bar{r}_B^2 = \langle \rho_B^2 \rangle$ .

When the different particles attract each other, i.e.  $a_{AB} < 0$ , the effective potential only has the minimum for coinciding centers where  $r = 0$ . The structures are then similar to those of one-component systems. Therefore, we shall here concentrate on the different structures appearing for repulsive cases where  $a_{AB} > 0$ .

The average sizes corresponding to Fig. 1 are shown in Fig. 2. For the minimum at  $r = 0$  we obtain large sizes, i.e.  $\bar{r}_A \approx \bar{r}_B \approx \bar{r} \approx 3b_t$ . This structure again closely resembles the one-component system. For a given division  $N_B/N_A$  both subsystems contract and stabilize on

a lower level as  $r$  increases to a few times the trap length. The smaller the system, the larger the contraction.

The effect of the repulsion is that the two systems try to avoid each other while staying at relatively small distances as dictated by the external field. The large subsystem ( $A$ ) is exploiting the space almost like it was alone in the trap. When one subsystem ( $B$ ) is small, it becomes advantageous to place about half of its particles outside the other subsystem. Then the repulsion on  $B$  from the trap and the subsystem  $A$  is minimized.

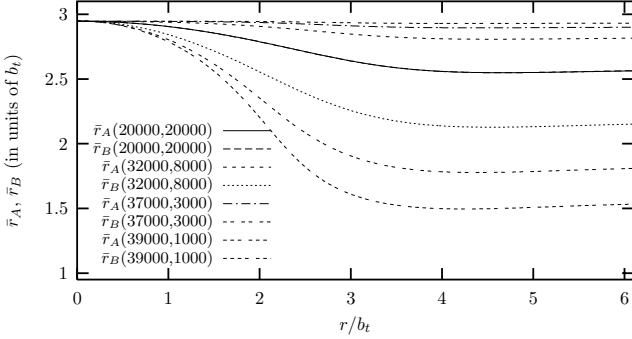


FIG. 2: The root-mean-square radii  $\bar{r}_A$  and  $\bar{r}_B$  as a function of  $r$  for the systems specified in Fig. 1.

The minima of the effective potentials define the preferred structure. As  $N_B/N_A$  changes, the system with the largest particle number ( $N_A$ ) always has the same size of about  $3b_t$  in these minima. In contrast, the size of the other subsystem decreases after  $N_B < 0.134N_A$  where the lower minimum at finite  $r$  appears. The values of  $\bar{r}_B$  converge towards  $b_t$  when  $N_B/N_A \rightarrow 0$ .

The center of mass of the small system ( $B$ ) remains within the radius  $\bar{r}_A$  until  $N_B \approx 0.004N_A$ . For even smaller subsystems the center of  $B$  moves a little outside  $\bar{r}_A$ , but still the distance between the centers at the minimum remains smaller than  $\bar{r}_A + \bar{r}_B$ . Therefore, complete separation between the systems does not occur.

*Stability.* The stability of the system is guaranteed for repulsion within both subsystems, i.e. when  $a_A > 0$  and  $a_B > 0$ . Instability arises for attraction where one or both subsystems can collapse into high-density states of lower energy. In Fig. 3 we illustrate these stability regions for a specific system as a function of the scattering lengths  $a_A = a_B < 0$  and  $a_{AB}$ . The results are extracted from the effective potential in Eq. (10). Stability is defined as the existence of a local minimum. We first consider  $r = 0$  and search for minima by variation of  $\rho_A$  and  $\rho_B$ . No stationary point exists for  $N_A = N_B$  when

$$\frac{N_A(a_A + a_{AB})}{b_t} \leq -\frac{2^{3/2}\pi^{1/2}}{5^{5/4}} \approx -0.67, \quad (12)$$

which follows the critical stability line in Fig. 3 for negative  $a_{AB}$ -values.

Maintaining  $r = 0$  we find that any stationary point of  $U_{eff}$  has negative curvature (second derivative) in one of

the principal directions when

$$\frac{a_{AB}}{b_t} \leq -\frac{5^5 N_A^4}{2^8 \pi^2} \left(\frac{a_A}{b_t}\right)^5 + \frac{1}{4} \frac{a_A}{b_t}, \quad (13)$$

$$\frac{N_A a_A}{b_t} \leq -\frac{2^{3/2}\pi^{1/2}}{5^{5/4}} \approx -0.67, \quad (14)$$

where Eq. (13) for  $0 < a_{AB}/b_t \lesssim 0.0001$  follows the critical stability curve in Fig. 3. Eqs. (12), (13), and (14) are comparable with the mean field approximation [8].

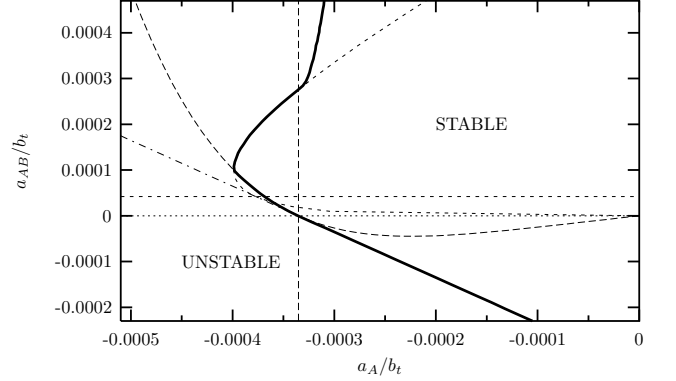


FIG. 3: Stability regions for a two-component system with  $N_B = N_A = 2000$  as a function of  $a_A = a_B < 0$  and  $a_{AB}$ . The thick solid line separates stable (right side) from unstable (left side) regions when we allow three degrees of freedom, i.e.  $\rho_A$ ,  $\rho_B$  and  $r$ . The different curves are related to Eqs. (12) (dotted), (13) and (14) (long-dashed), (15) and (16) (short-dashed), respectively.

When  $0.0001 \lesssim a_{AB}/b_t$ , the minimum of  $U_{eff}$  occurs for finite  $r$ , i.e. separation of the center of masses is favorable. Furthermore, the curvature at  $r = 0$  in the  $r$ -direction is negative when

$$\frac{a_A}{b_t} \leq \frac{a_{AB}}{b_t} - \frac{\pi^{2/5}}{2^{1/5} N_A^{4/5}} \left(\frac{a_{AB}}{b_t}\right)^{1/5}, \quad (15)$$

$$\frac{N_A a_{AB}}{b_t} \geq \frac{\pi^{1/2}}{2^{3/2} 5^{5/4}} \approx 0.084, \quad (16)$$

where Eq. (15) is decisive by defining the critical stability curve in Fig. 3 for  $0.0001 \lesssim a_{AB}/b_t \lesssim 0.00028$ . Eq. (16) resembles the mean-field expression derived in [9].

The critical stability curve is in agreement with mean-field computations for  $a_{AB}/b_t \lesssim 0.0001$ , but strongly deviating for  $0.0001 \lesssim a_{AB}/b_t$  where the system exploits the  $r$ -degree of freedom and becomes unstable for a range of attractive  $a_A/b_t$ -values. This is illustrated in Fig. 4 for a set of scattering lengths where a very shallow local minimum is present for coinciding centers, i.e.  $r = 0$ . Along the line defined by  $\rho_A = \rho_B$  a maximum is found around  $20b_t$  and a minimum at  $48.4b_t$ . This degree of freedom is analogous to the one-component mean-field coordinate. The two-component mean-field coordinates are presumably similar to the use of  $\rho_A$  and  $\rho_B$  for  $r = 0$ . A more detailed comparison is required to distinguish.

Moving now in the direction where the sum of  $\rho_A$  and  $\rho_B$  is constant and the difference varies, we find rather small barriers for  $(\rho_A, \rho_B) \approx (40b_t, 50b_t), (50b_t, 40b_t)$ . This degree of freedom is analogous to the two-component mean-field coordinates. We now decrease the repulsive scattering length  $a_{AB}$  by a factor of two from the value in Fig. 4 while maintaining  $a_A$ . Then the shallow minimum disappears in agreement with the Fig. 3 where the decrease of  $a_{AB}$  corresponds to crossing the curve described in Eq. (13) where one curvature changes sign. The larger repulsion in Fig. 4 stabilizes the system as predicted in the mean-field approximation. However, if the  $r$ -degree of freedom also is allowed, the system collapses by moving the centers apart from each other as described by Eq. (15). The local minimum in Fig. 4 is in fact unstable. Stability is regained for a finite  $r$ -value when  $a_A$  is less attractive and  $a_{AB} > 0.00028b_t$ , see the upper middle part of Fig. 3.

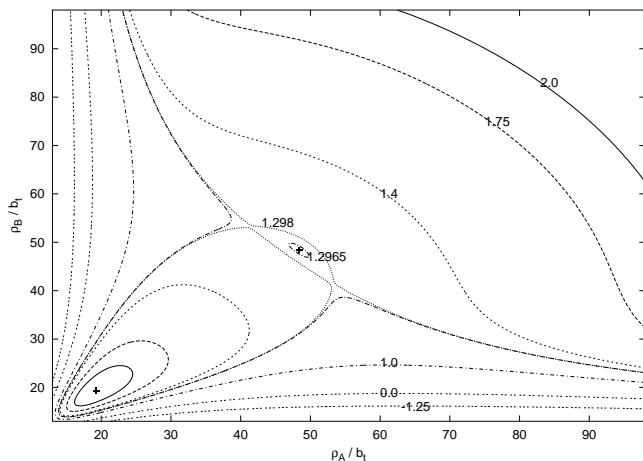


FIG. 4: Contour plot of the potential  $U_{eff}/(N\hbar\omega)$  in Eq. (10) as a function of  $\rho_A$  and  $\rho_B$  for  $r = 0$ ,  $N_A = N_B = N/2 = 2000$ ,  $a_{AB} = 0.0002b_t$ , and  $a_A = a_B = -0.00042b_t$ .

The critical line for stability of each of the independent systems  $A$  and  $B$  is also shown in Fig. 3 as  $a_A/b_t = -0.67/N_A = -0.00034$ . The repulsion between  $A$  and  $B$  stabilizes the total system even when each component would collapse when left alone. The reason is that the contraction of each subsystem increases the mutual repulsion. The balance of these forces results in

increased stability of the total system for moderate repulsion. In contrast, less stability results for strong repulsion where the collapse proceeds by circumventing the individual barriers via relative center-of-mass motion.

The two minima in Fig. 1 are not found when  $a_A = a_B$  and  $N_A = N_B$ . This feature only seems to occur for asymmetric systems. When both minima are present, each corresponds to a stable configuration. The vibrational zero-point energy is much smaller than the hardly visible, but stabilizing barrier in Fig. 1. Furthermore, estimates of the WKB tunneling probability show decay rates much smaller than the frequency of the external harmonic field. Co-existing structures are then possible.

*Conclusion.* We have investigated coupled two-component boson systems in a confining trap. The degrees of freedom are the sizes of the two components and the center-of-mass distance. Two new features emerge. First, new stable structures appear in the trap when identical and different pairs of bosons all repel each other and one of the components at the same time has many more particles than the other. Then a finite distance between the centers of the two components is energetically favored and two stable co-existing structures are possible.

The second new feature appears when identical bosons attract each other and different bosons repel each other. Some structures previously computed to be stable in the mean-field approximation are unstable. In the present model with more degrees of freedom, when the repulsion is sufficiently strong, the mean-field minimum becomes unstable against relative motion of the distance between the two centers of masses. The mean-field regions of stability are then further restricted.

The inaccuracies in the computations are all related to the choice of parameter space. Improving by including two-body correlations is possible for example by increasing the variational space of the wave function as done in [11, 12] for a one-component system. These improvements are then correspondingly expected to be substantial for hyperradii down to the range of the interaction, relatively small for hyperradii corresponding to condensate distances, and insignificant for larger distances. Thus the qualitative structure would remain unchanged and at the crucial distances for condensate formation the results are rather close to being quantitatively correct.

- 
- [1] C. J. Pethick and H. Smith, *Bose-Einstein Condensation in Dilute Gases* (Cambridge University Press, Cambridge, 2002).
  - [2] L. Pitaevskii and S. Stringari, *Bose-Einstein Condensation* (Clarendon Press, Oxford, 2003).
  - [3] C. J. Myatt, E. A. Burt, R. W. Ghrist, E. A. Cornell, and C. E. Wieman, Phys. Rev. Lett. **78**, 586 (1997).
  - [4] D. S. Hall, M. R. Matthews, J. R. Ensher, C. E. Wieman, and E. A. Cornell, Phys. Rev. Lett. **81**, 1539 (1998)
  - [5] P. Maddaloni, M. Modugno, C. Fort, F. Minardi, and M. Inguscio, Phys. Rev. Lett. **85**, 2413 (2000).
  - [6] G. Modugno, M. Modugno, F. Riboli, G. Roati, and M. Inguscio, Phys. Rev. Lett. **89**, 190404 (2002).
  - [7] A. G. Truscott, K. E. Strecker, W. I. McAlexander, G. B. Partridge and R. G. Hulet, Science **291**, 2570 (2001).
  - [8] Th. Busch, J. I. Cirac, V. M. Pérez-García, and P. Zoller, Phys. Rev. A **56**, 2978 (1997).

- [9] P. Öhberg, Phys. Rev. A **59**, 634 (1999).
- [10] B. D. Esry and Chris H. Greene, Phys. Rev. A **59**, 1457 (1999).
- [11] O. Sørensen, D.V. Fedorov and A.S. Jensen, J. Phys. **B** **37**, 93 (2004).
- [12] O. Sørensen, D.V. Fedorov and A.S. Jensen Phys. Rev. A **66**, 032507 (2002).
- [13] J. L. Bohn, B. D. Esry, and C. H. Greene, Phys. Rev. A **58**, 584 (1998).